Meta Heuristic Fusion Model for Classification with Modified U-Net-based Segmentation

Sri Laxmi Kuna[1], Dr. A.V. Krishna Prasad[2], Suneetha Bulla[3]
Research Scholar, Department of CSE, Koneru Lakshmaiah Educational Foundation, Amaravathi, India[1]
Research Supervisor, Department of CSE, Koneru Lakshmaiah Educational Foundation, Amaravathi, India[2, 3]

***Abstract*—General cause of diabetes mellitus is Diabetic Retinopathy (DR), which outcomes in lesions on the retinas that impair vision. If it is not detected in time, the result is severe blindness issues. Regrettably, there is no treatment for DR. Early diagnosis and treatment of DR can greatly lower the risk of visual loss. In contrast to computer-aided diagnosis methods, the manual diagnosis of DR using retina fundus images is more time-consuming effort, and high cost as well, as it is highly prone to error. Deep learning has emerged as one of the most popular methods for improving performance, particularly in the classification and analysis of medical images. Therefore, a deep structure-based DR detection and severity classification has been demonstrated for treating the DR with the usage of fundus images. The major aim of this developed technique is to classify the severity level of the retinal region of the human eye from the fundus images. At first, the required retinal fundus images are collected from the standard benchmark data sources. Secondly, image enhancement techniques are applied to the collected fundus images to improve the quality of images. Thirdly, the abnormality segmentations are carried out by using the optic disc removal process using active contouring model and then, the regional segmentation is done via the Modified U-Net method. Finally, the segmented image is subjected to the hybrid classifier network named a Hybrid Soft Attention-based DenseNet with Multi-Scale Gated ResNet (HSADMGR Net) for classifying the retinal fundus images and finding the severity level of the retinal images with higher accuracy. Furthermore, the parameters present inside the hybrid classifier network are optimized with the help of implemented Multi-Armed Bandits Groundwater Flow Algorithm (MABGFA). The test results regarding the developed deep structure-based DR model are validated with the existing DR detection and classification approaches by using different performance measures.**

Keywords*—Diabetic retinopathy segmentation and classification model; multi-armed bandits groundwater flow algorithm; hybrid soft attention-based DenseNet with multi-scale gated ResNet; modified U-Net-based segmentation

I. Introduction

One of the major issues facing people nowadays is diabetes. DR is one of the blindness diseases and it is complicated by diabetes. It has varying degrees of severity and it is hard to predict the DR in its early condition [9]. The retina, which converts light into the electric signal that is processed to produce an image, is impacted by DR. A network of abnormalities found in the retina gives nutrients to the retina. Abnormalities are damaged as a result of diabetes [10]. At that time, the retina does not contain a blood supply. This has an impact on retinal health and ultimately skews a person's vision [11]. Background retinopathy refers to the initial DR stage. Diabetes affects the blood vessels in the early stage, which causes sight loss [12]. It's possible for the vessels to swell slightly and leak blood, fluid, or proteins. Ophthalmologists or skilled graders manually identify DR, which is costly [13]. Lesions caused by diabetic retinopathy are typically believed to be reversible and the illness can only grow more slowly [14].

Convolutional methods frequently use a DL architecture with millions of learnable parameters [15]. Train a large amount of data suffers from the over fitting issue. Although, very effective laser therapy does not completely cure vision impairment and highlights the necessity of an efficient screening model [16]. Despite this fact, the screening of diabetic retinopathy is successful. An unacceptable amount of diabetes patients do not have the annual eye exams that are advised by guidelines [17]. One of the most significant issues faced by ophthalmologists and diabetes providers today is identifying at-risk patients and enabling them to get therapeutic therapies in a timely manner [18]. DR continues to be the cause of acquired vision loss despite the availability of healthcare facilities and the development of several methods that improve early detection. Maintaining such a register will probably be difficult because of the difficulty in obtaining precise [19], frequently updated lists from primary care practitioners. Due to these difficulties as well as the anticipated size and breadth of such a project, federal funding would probably be needed and would be expensive [20] for the construction of a national diabetes registry that allows for broad population coverage. The long-term advantages must be underlined, however, as they are of the opinion that such a register would significantly lower the rate of blindness among diabetes patients [21].

Due to their capacity to extract and learn the most discriminative features at the pixel level, convolutional neural networks (CNNs), a subset of deep learning, produced effective deep models for DR grading [22,23]. In this study, we create a method for the automatic segmentation and classification of retinal fundus picture using a convolutional neural network based on the U-Net architecture. We use data sets with very high resolution images labeled pixel by pixel to train neural networks.

The performance of a model is strongly influenced by how it is optimized using a small set of fundus images [25].

The deep learning-based DR segmentation and classification system objectives are described below.

- To design a deep learning-based DR segmentation and classification system that effectively detects the DR disease at an early stage that is helpful for DR patients in the hospitals to prevent blindness effectively.
- To develop an effective Modified U-Net-based abnormality segmentation to effectively segment the DR disease abnormalities from the fundus images.
- To implement a MABGFA optimization to optimize the parameters from HSADMGR Net to maximize the classification performance of the suggested model in terms of accuracy and precision.
- To develop an effective HSADMGR Net-based classification with optimized parameters like resblock, hidden neuron count, activation function and to maximize precision and accuracy.
- To validate the performance of the developed deep learning-based DR segmentation and classification model with different performance metrics among various optimization strategies and baseline models.

The suggested deep learning-based DR segmentation and classification system is explained in the remaining sections. The explanation of conventional DR segmentation and classification algorithms and methods and their advantages and disadvantages are given in Section II. The research problem is stated in Section II. The developed DR segmentation and classification model developed algorithm, and dataset details are given in Section IV. The segmentation of the DR disease and the preprocessing explanations are given in Section V. Section VI explains the DR classification and the developed model's objective functions. The experimental setup and results are given in Section VII and Section VIII. The summarization of the conclusion is given in Section IX.

II. Literature Survey

In 2021 Saeed *et al*. [1] have proposed a new DR screening system using effective deep learning with fundus images. The low-to-high-level characteristics was taught through a deep learning model. Initially, the first layer of the deep learning model was re-initialized utilizing regions of lesions derived from fundus images. To extract discriminatory characteristics from the input of fundus images in an unsupervised way, they replaced the full layers that encoded features that were global in domain-specific. The model was adjusted, so the lower layers were easy to find the normal regions and local, regional features of the lesion. It reduces the over-fitting problem. A classification layer based on gradient boosting was added last. The 10-fold cross-analysis used to evaluate the suggested model on two difficult datasets showed higher performance than conventional techniques. It helped graders make quick decisions regarding to a therapist for therapy during the early screening of DR patients.

In 2020 Shankar *et al*. [2] have investigated a new DR classification and automatic detection system using a deep learning framework. The contrast level of the fundus image was enhanced during the pre processing stage by utilizing the new method. The required features from the segmented image were then extracted using the developed model and the classification was done by Multilayer Perceptron (MLP) model. To ensure the accuracy of the investigated technique, a number of experiments were conducted using the MESSIDOR DR Dataset. The results of these experiments showed the superiority of the suggested system to the conventional techniques.

In 2020 Qiao *et al*. [3] have designed a new hybrid CNN-based DR segmentation system. Using deep learning techniques that were accelerated by Graphics Processing Units (GPUs), it was possible to identify the DR disease in fundus images and segments them with high performance and little latency. It offered a computerized technique to help ophthalmologists classify the input of fundus images like severe, early, or moderate NPDR. A deep learning technique suggested for early diagnosis of DR is also capable of effectively segmenting the DR disease. Also, it showed high prediction accuracy.

In 2023 Wang *et al*. [4] have implemented a method for segmenting four different types of fundus lesions associated with DR simultaneously using Deep Convolution Neural Networks (DCNN) that was totally autonomous. They suggested a collaborative design consisting of a local branch and a contextual branch to take advantage of multi-scale image information. To efficiently and completely merge informative features from the two branches, new mechanism was suggested to fuse the maps. To further increase the accuracy of the lesion segmentation model, it needed to reduce the over fitting issue in the developed model. Three publicly available fundus datasets were used in extensive experiments, and their methodology yielded a mean AUC value for each dataset separately. The outcomes of the suggested model showed greater performance when compared to other exceeding competing strategies and other cutting-edge models.

In 2023 Zhang *et al*. [5] have suggested a new DR identification and classification using a deep learning approach by examining the correlations between unlabeled data. It was possible to see that the ability of the network to extract crucial features could be improved by a mechanism that fitted the information. Unlabeled data was just potentially valuable labeled data, and the samples could increase the system's effectiveness. In order to effectively use the vast amounts of unlabeled information for precise DR classification, they offered a new framework. They specifically suggested an attention approach to remove the incorrect regions and retrieve factors from various views of input images in the developed model. Additionally, depending on the chosen annotated samples, they developed model compared to execute unknown samples to enhance the possibility of unlabeled information. For two open datasets, the experimental results showed that their new framework achieved high effectiveness.

In 2019 Jebaseeli *et al*. [6] have investigated a new framework for retinal disease segmentation using a neural network. That framework recommended the neural network model for automatically creating vectors, deep learning was proposed for classification, and pre processing method was used to remove the unwanted details. The Firefly method was used to adjust the DLBSVM parameters. The suggested methods were evaluated using the DRIONS, DRIVE, STARE,

REVIEW, and HRF fundus imaging datasets. The outcomes showed that the proposed methods given enhanced segmentation due to sensitivity, specificity and accuracy.

In 2022 Kushnure *et al.* [7] have implemented a new architecture for classifying the DR disease using the U-Net approach. It changed the skip pathways utilizing feature fusion mechanisms and local feature reconstruction that represent the specific information in features. To represent the rich spatial information in the low-level features, they used the new module in the bottleneck layer to represent multi-scale features with different receptive fields. These modifications improved segmentation efficiency while decreasing the complex problem of model compared to existing techniques. Furthermore, the independent results confirmed the investigated system's robustness.

In 2018 Mansour *et al.* [8] have investigated an effective DR disease prediction using neural network-based hybrid optimization. That was done in consideration of deep learning to solve very sophisticated segmentation issues. Pre-processing, Principle Component Analysis (PCA) connected component analysis-based localization, adaptive learning-based region segmentation, a high feature extraction, and Linear Discriminate and feature selection were included in the DR system. The proposed DR model performed better with LDA feature selection than with FC7 features or PCA, according to simulation results using common KAGGLE fundus datasets. It also performed more accurately among FC7 features than with LDA features. A comparison with the SIFT technique-based DR feature extraction demonstrated that deep learning-based DR works better than SIFT-based DR.

III. Problem Statement

Most of the conventional diabetic retinopathy classification and segmentation models do not detect the disease in its early stage. It takes more a lot of time while predict the DR disease and it provides more economic cost. Hence, it is unaffordable to many researchers. To overcome these problems, most existing approaches have been designed for the DR segmentation system and advantages and disadvantages are shown in Table I. CNN [1] provides high classification accuracy. Also, it reduces computational complexity. But, it is hard to segment the retinopathy disease because of the complicated structure, fewer voxel intensity variation and highly variable shape and also, it increases the economic cost. SVM [2] gives robustness. Also, it improves the accuracy of lesion segmentation. Yet, it takes a lot of time to classify the disease of DR and also it suffers from Class imbalance during the training. DCNN [3] avoids over fitting problems. Also, it maximizes specificity, accuracy and sensitivity. Yet, it is hard to predict the various lesions regardless of their complex texture, form and small scale and also, it gives very less quality input images and poor performance in the final outcome. DCNN [4] gives strong efficacy. Also, it avoids vision deterioration. But, it is hard to detect the dark spots in retinal images at the early stage and also, and it gives less classification accuracy. MASL [5] reduces the model complexity. Also, it gives more reliable results. Yet, it does not find the local structures of the lesion and also, and it needs a huge amount of data for effective segmentation. TPCNN [6] effectively reduces the cataract progression in the early stage. Also, it reduces the risk of vision loss. Yet, it does not generate the vectors to predict the DR disease and also, and it takes more time. UNet-CNN [7] effectively predicts the dark lesions also and it effectively classifies the DR disease. But, it is difficult to predict the fine vascular structures and causes of skin infections. CNN-DNN [8] effectively solves the intricate segmentation issue. Also, it effectively predicts the DR disease in its early stage. But, it is highly time-consuming while predicting the DR disease and also, and it suffers from over fitting issues. Hence, this disadvantage arises to design an efficient diabetic retinopathy classification and segmentation system with advanced deep-learning techniques.

TABLE I. Features and Challenges of Existing DR Classification Models Utilizing Deep Learning

Author [citation]	Methodology	Advantages	Disadvantages
Saeed et al. [1]	CNN	It provides high classification accuracy. It decreases computational complex issue.	It is hard to segment the retinopathy disease because of the complicated structure, fewer voxel intensity variations and highly variable shape. It increases the economic cost.
Shankar et al. [2]	SVM	It gives robustness. It improves the accuracy of lesion segmentation.	It takes a lot of time to classify the disease of DR. It suffers from Class imbalance during the training.
Qiao et al. [3]	DCNN	It avoids over fitting issues. It maximizes specificity, sensitivity and accuracy.	It is hard to predict the various lesions regardless of their complex texture, form and small scale. It gives very less contrast images and poor performance in the final outcome.
Wang et al. [4]	DCNN	It gives strong efficacy. It avoids vision deterioration.	It is hard to detect the dark spots in retinal images at the early stage. It gives less classification accuracy.
Zhang et al. [5]	MASL	It reduces the model's complexity. It gives more reliable results.	It does not find the local structures of the lesion. It needs a huge amount of data for effective segmentation.
Jebaseeli et al. [6]	TPCNN	It effectively reduces the cataract progression in the early stage. It reduces the risk of vision loss.	It does not generate the feature vectors at low level to detect the DR disease. It takes more time
Kushnure et al. [7]	UNet-CNN	It effectively predicts dark lesions also. It effectively classifies the DR disease.	It is difficult to predict fine vascular structures. It causes skin infections.
Mansour et al. [8]	CNN-DNN	It effectively solves the intricate segmentation issue. It effectively predicts the DR disease in its early stage.	It is highly time-consuming while predict DR disease. It suffers from the over fitting issue.

IV. Implementation of Diabetic Retinopathy Classification Framework using Hybrid Deep Learning Network

A. Proposed Diabetic Retinopathy Classification Framework

The main challenges with the DR detection models are it does not detect small-scale lesions, low-contrast images, and ambiguous boundaries. Successful segmentation also requires color information because lesions and healthy tissues can seem to be the same when they are of the same color. In the conventional models, they are suffered from the above segmentation issue. Low sensitivity is another problem with the previous segmentation models. The early detection of DR is still difficult, though, for a number of reasons. The current DR screening procedure takes more time. No baseline model used today produces findings that are satisfactory outcomes, because they are frequently very small micro aneurysms and they are susceptible to misdiagnosis or being mistakenly categorized as hemorrhages. For a significant portion of the retinal image collection, some of them were difficult to detect. Because of their resemblance in the color of blood arteries and their proximity to them in some research studies, micro aneurysms are challenging to segment. The abnormality intersection characteristic has been employed in some approaches to derive the optic disc. However, the interference from the blood vessels, they use the entire abnormality structure, which may produce inaccurate or inconclusive results. As a result, the majorities of studies using various image processing methods have not reached a high level of accuracy and fail to categorize the DR disease. The investigated deep learning-based disease of DR segmentation and classification model is shown in Fig. 1.

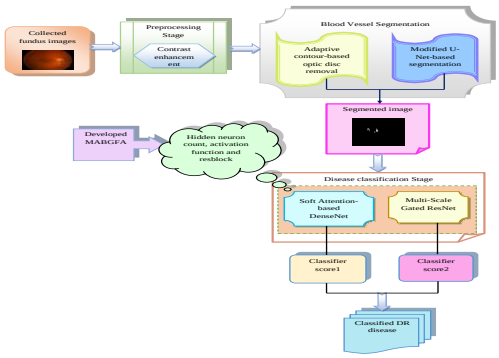

Fig. 1. Proposed deep learning-based DR segmentation and classification model.

The newly designed DR segmentation and classification model using new technique to predict the disease in its early stage. It helps in hospitals to prevent vision loss or blindness for patients. It effectively predicts the retinal thin outer structure. The retinal fundus images are collected using the internet resources. The collected fundus images are given to the next stage. Here, the pre processing can be done utilizing a contrast enhancement approach [36]. The pre-processed retinal images are given to the segmentation section. Here, the two types of segmentation process such as abnormality segmentation and regional segmentation can be segmenting the pre processed images. The abnormality segmentation can be performed using Adaptive contour-based optic disc removal process [24]. The regional segmentation can be performed using Modified U-Net method technique. After, the segmentation the images are undergoes the next stage. The classification can be done using HSADMGR Net technique. Here, the investigated MABGFA optimization used for optimizing the parameters that is activation function, hidden neuron count and resblock to maximize the precision and accuracy. The designed HSADMGR Net-based DR

Segmentation and classification system performance is validated to other traditional methods and heuristic algorithms in terms of a number of performance measures.

B. Dataset Details

The collected fundus images are gathered through the benchmark dataset using the below link "https://www.it.lut.fi/project/imageret/diaretdb1/. This dataset contains normal and diseased retinal images. It also contains 89 types of color fundus images. Here, the fundus images are gathered using 50 degree view of workable camera. This dataset give a better accurate solution during DR detection. The model's primary goal was to clearly describe a database and a testing procedure that can be used to compare various DR detection techniques. Hence, the collected retinal fundus images are denoted by A_q^{Np}, where $q = 1,2,\cdots,Q$. The total numbers of sample images are indicated by N. The collected fundus images adopted for the DR segmentation and classification system are shown in Fig. 2.

Dataset specification	Sample 1	Sample 2	Sample 3	Sample 4	Sample 5
Normal retinal images	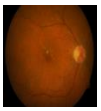	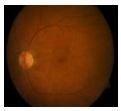		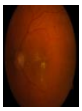	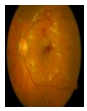
Diseased retinal images	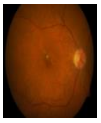		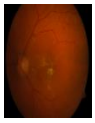	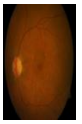	

Fig. 2. Gathered fundus images from the dataset for the segmentation and classification of DR diseases.

C. Proposed MABGFA

The developed MABGFA optimization is adopted to improve the effectiveness of the deep learning-based DR classification and segmentation model with the help of optimized the parameters such as hidden neuron count, activation function, and resblock for maximizing accuracy. The MABOS algorithm is simple to understand and simple to use. But, it continues to experience problems such as unequal exploitation, lack of diversity, and local optimum. It is simple to fall into an optimal local situation in high-dimensional space. The GFA algorithm increases computing effectiveness and control parameter resilience. But, the convergence rate is poor. That takes a huge amount of time to finish. The GFA algorithm suffers from processing vast amounts of data in order to produce superior results. The implementation is also very challenging. So, they developed MABGFA optimization is adapted to segment and classify the disease from fundus

images. The MABGFA optimization is designed related to mean, worst and best fitness functions. Here, the random number to be distributed is indicated by *rnd* . In the traditional optimization, the term *rnd* is chosen in the interval of [0,1]. But, in the developed algorithm, it is estimated using Eq. (1).

$$rnd = \frac{\sqrt{worstfit} + \sqrt{meanfit}}{besfit} \tag{1}$$

The best fitness is represented as *besfit* and the worst fitness value is indicated by *worstfit* . The term *meanfit* indicates the mean fitness value. By using this newly estimated value, this algorithm converges very fast and gives superior optimization results in the solution space.

MABOS [26]: The balance between exploration and exploitation is crucial in the classic reinforcement learning problem known as Multi-Armed Bandits (MAB). Here, various utility qualities are used that are named armed bandits. Initially, there is no prior knowledge of bandits. The resource is fixed and limited, which can be seen in terms of computing time. When they provide the bandit's resources, the objective is to decrease the regret or increase the gain. The estimated parameter is denoted by R . The true-action parameter is denoted by r . The term b is the selected action. The expected reward is calculated using Eq. (2).

$$r(u,b) = F[S(u)B(u)] = b \tag{2}$$

Here, the iteration count is denoted by u . The term $B(u) = b$ indicates the selected action. The current reward is indicated by $S(u)$. The term $B^*(u)\arg\max_b R(u,b)$ indicates the greedy action. It is measured using $R(u,b)\alpha r(u,b)$. The optimal value is calculated using Eq. (3).

$$w^*(u) = r(b^*,u) = \max_{b\in B} r(b,u) \tag{3}$$

The opportunity loss is calculated by the total number of regret and it is given in Eq. (4).

$$M_U = F\left[\sum_{u=1}^{U}\left(w^*(u) - r(b(u),u)\right)\right] \tag{4}$$

Hence, regret is unavoidable because they can't always choose the best action. If the system changes to smooth, they anticipate the estimation to get more accurate results. Initially, the action is chosen for every time and, a reward is collected, the evaluation of the action value is updated. The term b is denoted by the action operator and it is chosen by using the number of times parameter $O_u(b)$. It is given in $g(S_1, S_2, ..., S_{O_u(b)})$. The achieved rewards are measured by the term R and it is given in $R(u,b) = \sum_{j=1}^{O_u(b)} S_j / O_u(b)$. Using the non-stationary and stationary measures the updated increment is calculated using Eq. (5).

$$R(u+1,b) = (\beta)R(u,b) + (1-\beta)S(u) \tag{5}$$

Here, the term hyper parameter is denoted by β and it is selected using $(\beta \in [0,1])$. Smaller values of β are suitable for dynamic systems because they focus more on recent rewards. On the other hand, choosing a small value β relies on the present reward. Hence, choosing this parameter requires better balance. The experiments section includes the value of β and this value is utilized for this algorithm.

The main issues with this problem are known to be the most crucial part of MAB to maintain the balance between the exploration for improved estimates and unreliable estimates in exploitation. It is used to increase the regret with the low cost. In this algorithm, the action uncertainty is considered to determine the expected value. The term *VDC* is measured using Eq. (6).

$$VDC(u,b) = R(u,b) + dV(u,b) = R(u,b) + d\sqrt{\frac{L(u)}{M_u(b)}} \tag{6}$$

Here, the hyper parameter is denoted by d and it increases the confidence level of the upper bound in final validation. The non-negative real value is indicated by d and it decreases the uncertainties in the final validation. The term $soft\max$ is used for selecting the *VDC* action easily, and it is measured using in Eq. (7).

$$Q(B = b) = soft\max(VDC(b)) = \frac{\exp[VDC(b)]}{\sum_{b\in B}\exp[VDC(b)]} \tag{7}$$

The fitness value is increased using the term L . If the condition is $d = 0$ they do not change the final process. Balance is based on the selection of values. The term Q gives the best solution using the upper confidence actions and better-estimated value.

GFA [27]: In the suggested optimization technique and traveling multiple paths in search of a solution is the crucial issue. The dimension is indicated by E . The GFA gives the best solution. The GFA initialization is given in Eq. (8).

$$y_{jk} = mc_k(g) + rnd_k(1)\times(vc_k(g) - mc_k(g)) \tag{8}$$

The candidate solution is denoted by y_{jk} . The term *rnd* indicates the random number. Every candidate solution is determined by using the velocity. Every GFA velocity is assigned to 0 and it is given in Eq. (9).

$$w_j(\vec{0}) = 0 \tag{9}$$

Here, the initial velocity is indicated by $w_j(\vec{0})$. The terms $E\vec{B}_j(u)$ and $M\vec{B}_j(u)$ are calculated using Eq. (10) and Eq. (11), respectively.

$$E\vec{B}_j(u) = rnd_j\left(E\vec{B}_1(u), E\vec{B}_1(u), ..., E\vec{B}_h(u)\right),$$
$$h = flr\left(\frac{Q\times o}{100}\right) \tag{10}$$

$$M\vec{B}_j(u) = mean\left(y_k^{\rightarrow}(u)\right) \forall k \quad (11)$$

Here, the selected value of EB is indicated by $E\vec{B}_j(u)$. The term $M\vec{B}_j(u)$ denotes the local average value of GFA. The ratio calculations of Δi_{je} and Δi_{jm} are measured using Eq. (12) and Eq. (13), respectively.

$$\Delta i_{je}^{\rightarrow}(u) = E\vec{B}_j(u) - y_k^{\rightarrow}(u) \quad (12)$$

$$\Delta i_{jm}^{\rightarrow}(u) = M\vec{B}_j(u) - y_k^{\rightarrow}(u) \quad (13)$$

Here, the terms e and m represents the subscripts of EB and MB, respectively. The terms $M_{je}(u)$ and $M_{jm}(u)$ are measured using Eq. (14) and Eq. (15), respectively.

$$M_{je}(u) = \frac{\max_{k \neq j} \left| g\left(y_k^{\rightarrow}(u)\right) - g\left(y_k^{\rightarrow}(u)\right) \right|}{\left| g\left(EBy_k^{\rightarrow}(u)\right) - g\left(y_k^{\rightarrow}(u)\right) \right|} \quad (14)$$

$$M_{jm}(u) = \frac{\max_{k \neq j} \left| g\left(y_k^{\rightarrow}(u)\right) - g\left(y_k^{\rightarrow}(u)\right) \right|}{\left| g\left(MBy_k^{\rightarrow}(u)\right) - g\left(y_k^{\rightarrow}(u)\right) \right|} \quad (15)$$

Darcy's law calculates the velocity and it is directly proportional to the term IH and it is calculated by Eq. (16) and Eq. (17), respectively.

$$IH_{je}^{\rightarrow}(u) = \frac{\Delta i_{je}^{\rightarrow}(u)}{M_{je}^{\rightarrow}(u)} \quad (16)$$

$$IH_{jm}^{\rightarrow}(u) = \frac{\Delta i_{jm}^{\rightarrow}(u)}{M_{jm}^{\rightarrow}(u)} \quad (17)$$

The term we is a discharge velocity. The coefficient factor is denoted by l. The discharge velocity is measured by Eq. (18) and Eq. (19), respectively.

$$we_{je}^{\rightarrow}(u) = l \times IH_{je}^{\rightarrow}(u) \quad (18)$$

$$we_{jm}^{\rightarrow}(u) = l \times IH_{jm}^{\rightarrow}(u) \quad (19)$$

Both discharge velocities of EB and MB are combined using Eq. (20).

$$we_j^{\rightarrow}(u) = \beta \times we_{je}^{\rightarrow}(u) + (1-\beta) \times we_{jm}^{\rightarrow}(u) \quad (20)$$

Here, the term β controls the water levels using the selected weight range in $[0,1]$. Water's discharge velocity is its speed when there is no barrier in its path. In general, groundwater travels via porous media called aquifers. Hence, the aquifers' pores are the only places where water can pass. The division of discharge velocity and the intermediate medium is known as velocity of seepage. The velocity of seepage is measured using Eq. (21).

$$wt_j^{\rightarrow}(u) = \frac{we_j^{\rightarrow}(u)}{\gamma_j} \quad (21)$$

The intermediate medium is denoted by γ. The dimension is updated using DG and it is indicated by e. The term DG is a controlling factor calculated by Eq. (22).

$$DG(u) = \left(1 - \frac{u}{U}\right) \times E \quad (22)$$

Here, the term U is the maximum number of iterations. The randomly selected integer is indicated by e. The dimensions are updated by Eq. (23).

$$\gamma_j = \frac{e_j}{E} \quad (23)$$

The velocity of $w_j^{\rightarrow}(u)$ is measured using Eq. (24).

$$w_j^{\rightarrow}(u) = \alpha \times w_j(\vec{u-1}) + \kappa \times wt_j^{\rightarrow}(u) \quad (24)$$

Finally, the velocity of any one GFA can be determined by adding its seepage velocity to its previous velocity. When all GFAs share the same fitness measures, the best solution can be found. The pseudo-code of the investigated MABGFA is given in Algorithm 1.

Algorithm 1: Designed MABGFA

```
Initialize the iterations U and population y_j
Load the initial positions
Calculate the initial fitness value
    Update the parameter rnd with the adaptive concept
  While (u ≤ U)
        For
    (j = 1to Maxiter)
    For (k = 1to pop)
        If (rnd < 0.5)
                    Update the parameter using MABOS in Eq. (9).
                    Evaluate the seepage velocity
        Else:
                    Update the parameter using GFA in Eq. (23).
        End if
        Calculate the discharge velocity
     End For
     Select the value using softmax sampled by Eq. (7).
     Validate the best fitness solution
  End while
  Return the parameters
End
```

V. Abnormality Segmentation and Regional Segmentation for Diabetic Retinopathy Classification using Fundus Images

A. Preprocessing of Fundus Images

The collected fundus images are given to the pre processing stage indicated by A_q^{Np} . Image enhancement is the technique of enhancing the original data images and details. Typical techniques add the density slicing, contrast enhancement and spatial filtering,. By applying a linear transformation, the original range of grey levels is expanded, resulting in contrast enhancement. The natural linear factors such as shear zones, lineaments and fault are improved by contrast enhancement. In order to indicate various aspects, density slicing breaks up the continuous intervals, each designated by a different color. The preprocessed image is denoted by A_m^{pre} .

B. Active Contour-based Optic Disc Removal

The preprocessed image A_m^{pre} is given in the segmentation section. The optical disk is eliminated from the inverted equalization image before it is given to element. It is used to open the edge-improved image based on curvelets in order to remove it. For the purpose of removing the optic disc, the morphological procedure is applied, which is used for the complete removal of the optic disk. The term $Dj - Tf$ defines the erosion process and it is calculated using Eq. (25).

$$Dj - Tf = \{W \in F / Ty \subseteq Dj\} \tag{25}$$

Here, the initial input is indicated by Dj . As a result, the term Ty is measured using Eq. (26).

$$Ty = \{g + y / g \in Tf\}, \forall_y \in F \tag{26}$$

The active contour is a recent method that divides the further analysis and processing using energy forces and challenges. The approach of collecting deteriorated structures from an image with respect to issues and energy forces for the segmentation of blood arteries is known as active contouring. The bounds of the image elements are decided by the contour model to produce a contour. Using a variety of approaches that include both internal and external forces, the structure's curvature is determined. The energy function is determined in order to acquire the required structure. To define contour deformations, a group of points that define a contour are used. As a result, the segmented image produced by active contouring is represented by KR_r^{out} .

C. Modified U-Net-based Abnormality Segmentation

The input given to the regional segmentation section is indicated by KR_r^{out} . The modified U-Net-based segmentation procedure will receive as its input. It is used to encode the fundus image using the Modified U-net encoder. The decoder contains number of U-Net blocks to given the output of the model. The output of the previous block is to be up sampled and activation features are sent from an intermediary layer of the encoder to each U-Net block.

Encoder and Decoder: The decoder and encoder are the two components that make up the modified U-Net. The encoder utilizes ResNet architecture that has already been trained. The residual network is primarily used because, when compared to other pre-trained models, it has a higher accuracy in image classification issues. It contains four blocks ReLu, decoder, encoder and batch normalization. There are four U-Net blocks in the decoder. The up sampling mechanism in the improved images convolution initialized to convolution block. The model's deconvolution layer has been swapped out for a sub-pixel convolution layer. Therefore, the segmented image produced by modified U-Net is represented by OT_s^{Bld} . The basic diagram of the Modified U-Net-based segmentation system is shown in Fig. 3.

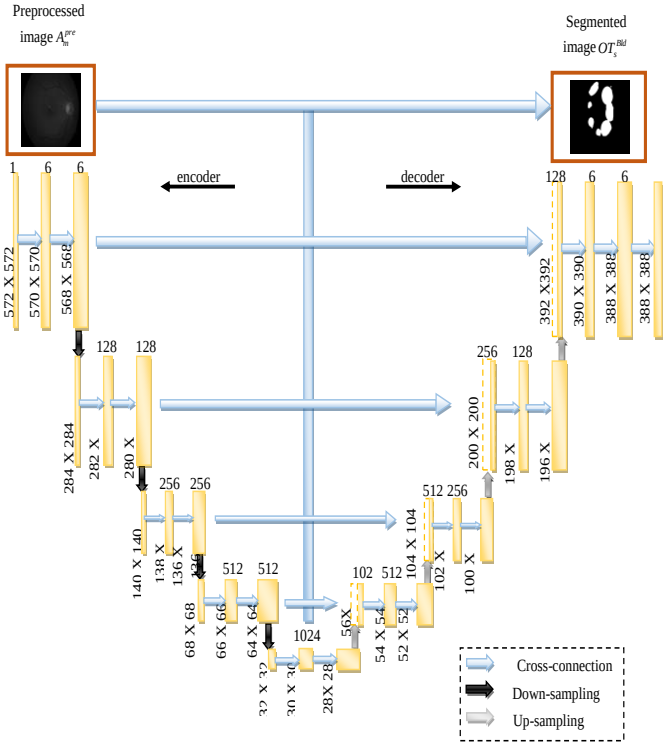

Fig. 3. Modified U-Net-based segmentation system.

VI. Classification of Diabetic Retinopathy using Hybridization of Soft Attention-based Densenet and Multi-Scale Gated Resnet

A. Soft Attention-based DenseNet

The segmented image given to the classification section is denoted by OT_s^{Bld} . The classification process is a one of the supervised learning technique. It adopted a data into different classes. It trained the models and predicts the groups.

DenseNet [29]: Transition and dense blocks are used to build the DenseNet model. The pooling layer is part of the Convolution unit in the transition block. The transition block is employed to eliminate the complexity of computation. The bottleneck layer used in the convolution reduces the input feature map sizes. Therefore, it minimizes the feature

mappings at transition layers. The transition stage receives the output.

Soft attention block: Soft attention increases the robust ssystem. It favors the most pertinent input while allowing a portion of the other data to influence the system's judgment. It is based on the precise location determined by the feature map that was extracted. The term T is a soft attention score and it is indicated by Eq. (27).

$$T = \sum_{L=1}^{L} \frac{\exp\left(g_{3e_{jk}}\right)}{\sum_{j=1}^{x^y}\sum_{k=1}^{i^y}\exp\left(g_{3e_{jk}}\right)},\ g_{3e} = I\left(g^y\right) \tag{27}$$

$$\beta_z = g^y + zg_t^y \tag{28}$$

This model is assisted in choosing the precise positions of the feature map's relevant properties by the finished soft attention layer.

B. Multi-Scale Gated ResNet

Multi-scale Gated model [32]: They develop an attention-gating module for the top-down adaptive fusion as opposed to the typical method of feature concatenation from several layers or multi-scale inputs. It directs the second level's learning through the gating operation, the fusion process begins. The hierarchical fusion operation is calculated using Eq. (29).

$$B_j = \beta\left(X^{7\times7}\left(\left[AvgPl\left(G_j\right), MaxPl\left(G_j\right)\right]\right)\right) \tag{29}$$

$$G_{j+1}^{`} = up\left(B_j\right) \circ C\left(G_{j+1}\right)\left(j = 1,2,3\right) \tag{30}$$

Finally, the gated feature at the top level includes both high-level semantic knowledge and high-resolution spatial data. The saliency map is normalized using a sigmoid activation function.

ResNet: The DR is primarily classified with the resnet technique. The block of the resnet is used to determine the direct residual output. The term $J(z)$ is a target output. The degradation happens much more quickly when there are multiple convolutional layers. The resnet has a lot of small connections that allow us to identify the mapping process indirectly by skipping one or two tiers. The residual mapping function is given in Eq. (31).

$$H = B_2\gamma\left(B_1 z\right) \tag{31}$$

Here, the term γ indicates the Relu activation function.

$$a = H\left(z, \{B_k\}\right) + z \tag{32}$$

Here, the term a is a representation of the second Relu's shortcut connection. Finally, they effectively predict the DR disease and also increase the performance of classification using res net.

C. Proposed HSADMGRNet-based Diabetic Retinopathy Classification

The HSADMGR Net-based system enhances the classification effectiveness over the segmentation and classification of DR with high accuracy. The designed MABGFA optimization is utilized for optimizing the parameters like res block, hidden neuron count and activation function. The HSADMGR Net model with MABGFA optimization maximizes the accuracy and precision of the designed DR segmentation and classification model. The Soft Attention-based DenseNet method improves classification accuracy. It takes less time to segment the DR disease. DenseNet replicates the data numerous times and splices the feature maps of each layer with the layer before. Sometimes it makes misdiagnosis results. A Multi-Scale Gated ResNet approach considerably reduces the error rate below a certain threshold, further enhancing the network. But, it takes weeks of segmentation, which makes it practically impossible to use in real-time. The computational density of the ResNet method is one of its main disadvantages. To resolve these problems, the suggested MABGFA-HSADMGR Net-based DR classification model is developed to enhance the classification results. The developed MABGFA-HSADMGR Net-based DR classification model gives better fitness in terms of maximization of accuracy and precision and it is given in Eq. (33).

$$Ob_j = \underset{\left\{\begin{array}{l} SA_{DesNet}^{Linear}, SA_{DesNet}^{sigmoid}, SA_{DesNet}^{\tanh}, SA_{DesNet}^{\mathrm{Re}\,Lu} \\ KJ_{\mathrm{Re}sNet}^{Linear}, KJ_{\mathrm{Re}sNet}^{sigmoid}, KJ_{\mathrm{Re}sNet}^{\tanh}, KJ_{\mathrm{Re}sNet}^{\mathrm{Re}\,Lu}, \\ KJ_{\mathrm{Re}sNet}^{Hidden}, KJ_{\mathrm{Re}sNet}^{resbk} \end{array}\right\}}{\arg\min} \left(\frac{1}{Ac} + \frac{1}{\mathrm{Pr}}\right) \tag{33}$$

Here, the optimized ReLu, linear, tanh and sigmoid activation functions from the DenseNet are denoted by $SA_{DesNet}^{\mathrm{Re}\,Lu}$, SA_{DesNet}^{Linear}, $SA_{DesNet}^{\tanh}$ and $SA_{DesNet}^{sigmoid}$ in the interval of $[0,3]$, respectively. The optimized ReLu, linear, tanh and sigmoid activation functions from the ResNet are indicated by $KJ_{\mathrm{Re}sNet}^{\mathrm{Re}\,Lu}$, $KJ_{\mathrm{Re}sNet}^{Linear}$, $KJ_{\mathrm{Re}sNet}^{\tanh}$ and $KJ_{\mathrm{Re}sNet}^{sigmoid}$ in the interval of $[0,3]$, respectively. The hidden neuron count from ResNet is indicated by $KJ_{\mathrm{Re}sNet}^{Hidden}$ and it is selected in the interval of $[5,255]$. The optimized res block in the ResNet is indicated by $KJ_{\mathrm{Re}sNet}^{resbk}$ and it is selected in the interval of $[3,15]$. The precision parameter is calculated using Eq. (34).

$$PR = \frac{UO_f}{UO_T + UF_m} \tag{34}$$

The accuracy is measured using Eq. (35).

$$A = \frac{\left(UO_T + UF_p\right)}{\left(UO_T + UF_p + UO_f + UF_m\right)} \tag{35}$$

The true positive and negative values are denoted by UO_T and UO_f, respectively. The false positives and false negatives are indicated by UF_p and RU_s, respectively. A diagrammatic representation of the developed MABGFA-HSADMGR Net-based DR classification is shown in Fig. 4.

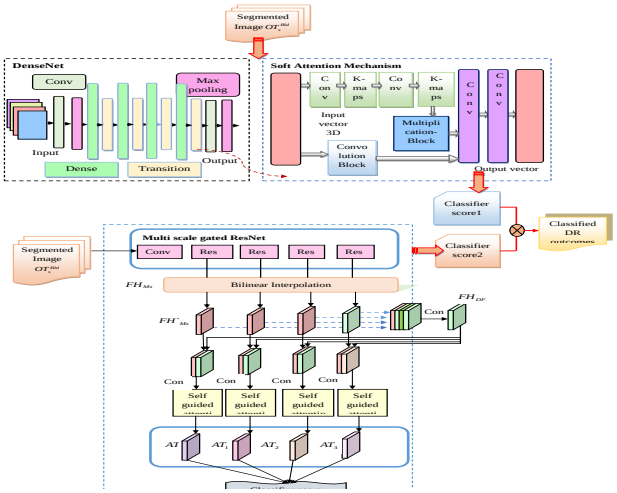

Fig. 4. MABGFA-HSADMGR Net-based DR classification system.

VII. Results and Discussions

A. Experimental Setup

The developed MABGFA-HSADMGR Net-based DR segmentation and classification model was developed by using Python environment. The performance of the DR segmentation and classification model was validated over different classification methods and hybrid algorithms via many evaluation measures. The analysis was conducted using a population rate of 10, an iteration gap of 10 and a chromosomal length of 5. For validation, classifiers including Mobile Net [28], Dense net [29], VGG16 [30], XGBOOST [31], MG_Res Net [32], and RN-Bi-LSTM [33] were considered and several optimization algorithms like Harris hawks optimization (HHO) [34], Salp Swarm Algorithm (SSA) [35], MABOS [26], and GFA [27] were utilized.

B. Pre-Processing and DR Segmentation Output

The outputs of the Modified U-Net-based DR disease segmentation system are given in Fig. 5. The segmentation performed utilizing the Modified U-Net approach.

Description	Sample1	Sample 2	Sample 3	Sample 4	Sample 5
Original retinal images	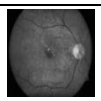	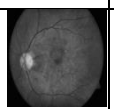			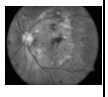
Pre-processed retinal images	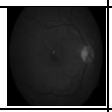	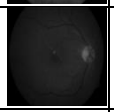	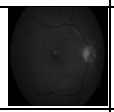	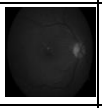	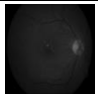
Modified U-Net-based Segmented retinal images					

Fig. 5. Outcomes of the designed Modified U-Net-based DR segmentation.

C. Evaluation Measures

The effectiveness measures used for the implemented DR segmentation and classification model are described as below.

a) FNR: The FNR is measured by Eq. (36).

$$FNR = \frac{UO_T}{UF_p + UF_m} \tag{36}$$

b) NPV: It is measured using Eq. (37).

$$NPV = \frac{UF_p}{UF_p + UO_m} \tag{37}$$

c) Sensitivity: It is validated using Eq. (38).

$$SEN = \frac{UF_m}{UF_m + UO_f} \tag{38}$$

d) FPR: The FPR is calculated using Eq. (39).

$$FPR = \frac{UF_p}{UF_p + UO_f} \tag{39}$$

e) F1-score: The F1-score value is measured using Eq. (40).

$$F1 = \frac{2 \times UF_m}{2UF_m + UO_f + UO_T} \tag{40}$$

f) MCC: The MCC value is calculated by Eq. (41).

$$MCC = \frac{UO_T \times UO_f - UF_m \times UF_p}{\sqrt{(UO_T + UF_m)(UO_T + UF_p)(UO_f + UF_m)(UO_f + UF_p)}} \tag{41}$$

g) FDR: it is measured by Eq. (42).

$$FDR = \frac{UF_p}{UF_p + UO_T} \tag{42}$$

h) Specificity: The specificity is measured by Eq. (43).

$$SP = \frac{UO_f}{UO_f + UF_m} \tag{43}$$

VIII. Result Analysis

A. Performance Analysis of the Developed DR Segmentation and Classification Model with respect to Learning Percentage

Performance comparison of the developed MABGFA-HSADMGR Net-based DR segmentation and classification system to conventional techniques and hybrid algorithms is shown in Fig. 6 and Fig. 7, respectively. Then, the developed MABGFA-HSADMGR Net-based DR segmentation and classification system improved with a high sensitivity of 18% more than Mobile Net, 16.6% more than Dense Net, 15.2% more than VGG16, 12.6% than XGBOOST, 8.8% than MG_Res Net and 7.6% than RN-Bi-LSTM with the value of learning percentage is 35. As a result, the designed MABGFA-HSADMGR Net-based DR segmentation and classification model has achieved better classification rates when compared to conventional techniques and heuristic strategies.

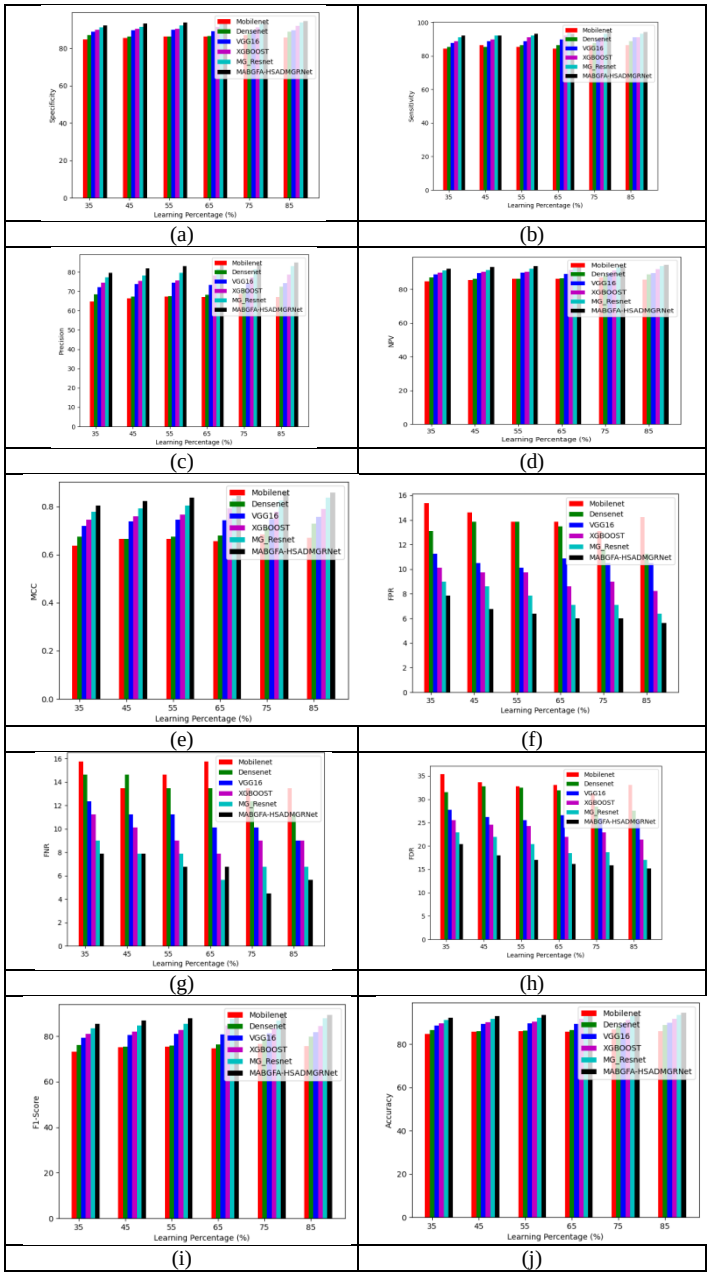

Fig. 6. Performance validation of various heuristic algorithms in terms of "(a) Specificity, (b) Sensitivity, (c) Precision, (d) NPV, (e) MCC, (f) FPR, (g) FNR, (h) FDR, (i) F1-Score, and (j) Accuracy".

B. Performance Analysis of the Developed Model with respect to Epochs

A performance comparison of the developed MABGFA-HSADMGR Net-based DR segmentation and classification model to existing techniques and algorithms to existing techniques and algorithms in terms of epoch analysis is shown in Fig. 8, and Fig. 9, respectively. In the Epoch value of 100, the developed MABGFA-HSADMGR Net-based DR segmentation and classification showed a high precision of 18.6% more than Mobile Net, 18.1% more than Dense Net, 18.1% than VGG16, 15% than XGBOOST, 13% than MG_Res Net and 12% than RN-Bi-LSTM. Therefore, the designed MABGFA-HSADMGR Net-based DR segmentation and classifications system has achieved high efficacy due to accuracy.

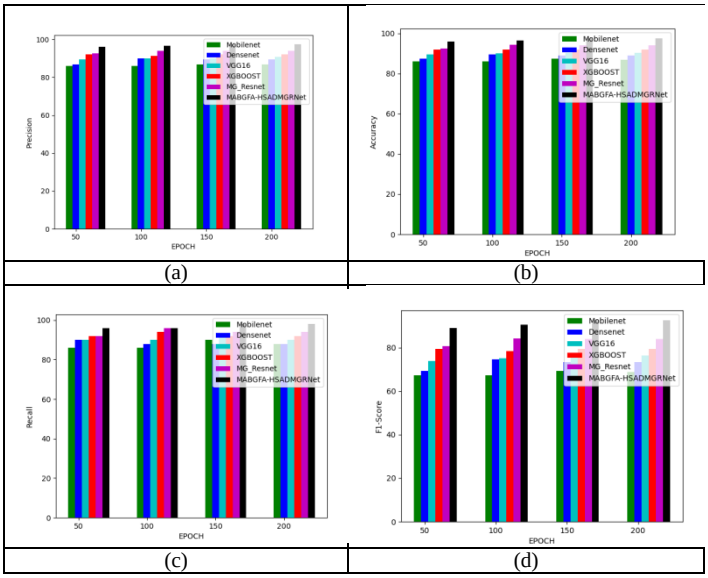

Fig. 7. Performance analysis of over various techniques in terms of "(a) Precision, (b) Accuracy, (c) Recall, (d) F1-Score".

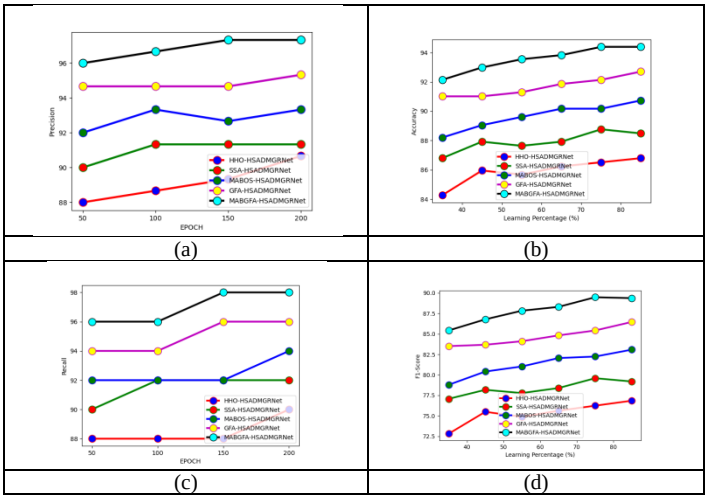

Fig. 8. Performance analysis of over different heuristic algorithms in terms of "(a) Precision, (b) Accuracy, (c) Recall, (d) F1-Score".

C. Cost Function Analysis of the Developed DR Classification and Segmentation System

A performances comparison of the developed MABGFA-HSADMGR Net-based DR segmentation and classification system to previous classification techniques and hybrid algorithms to existing techniques and algorithms in terms of cost function analysis is shown in Fig. 6. In the value of 5, The developed MABGFA-HSADMGR Net-based DR segmentation and classification showed with cost function of 4.4% than HHO-HSADMGR Net, 4.2% than SSA-HSADMGR Net, 3.8% than MABOS-HSADMGR Net, 4.1% than GFA-HSADMGR Net. Therefore, the designed MABGFA-HSADMGR Net-based DR segmentation and classification model has showed high efficacy.

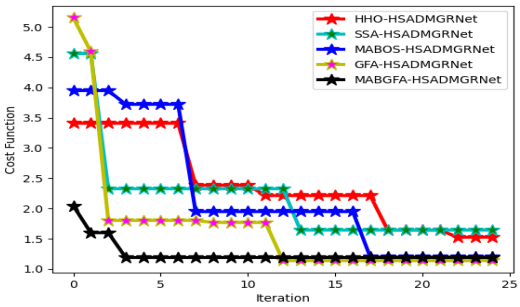

Fig. 9. Cost function analysis of suggested DR classification and segmentation model among different heuristic algorithm.

D. Overall Validation of the Implemented DR Segmentation and Classification System

The newly designed MABGFA-HSADMGR Net-based DR segmentation and classification model performance is analyzed using various heuristic algorithms and existing methods, shown in Table II and Table III, respectively. The developed DR classification and segmentation model has improved the f1-score of 3.4% than HHO-HSADMGR Net, 7.2% than SSA-HSADMGR Net, 9.8% than MABOS-HSADMGR Net, 14.1% than GFA-HSADMGR Net. The developed model performed more accurately and efficiently over previous hybrid algorithms and existing methods.

TABLE II. PERFORMANCE ANALYSIS OF DR SEGMENTATION AND CLASSIFICATION SYSTEM WITH HEURISTIC ALGORITHM

Terms	HHO-HSADMGR Net [28]	SSA-HSADMGR Net[29]	MABOS-HSADMGR Net[30]	GFA-HSADMGR Net[31]	MABGFA HSADMGR Net
Accuracy	86.51685	88.76404	90.16854	92.13483	94.38202
Sensitivity	86.51685	87.64045	91.01124	92.13483	95.50562
Specificity	86.51685	89.13858	89.88764	92.13483	94.00749
Precision	68.14159	72.8972	75	79.61165	84.15842
FPR	13.48315	10.86142	10.11236	7.865169	5.992509
FNR	13.48315	12.35955	8.988764	7.865169	4.494382
NPV	86.51685	89.13858	89.88764	92.13483	94.00749
FDR	31.85841	27.1028	25	20.38835	15.84158
F1-Score	76.23762	79.59184	82.2335	85.41667	89.47368
MCC	67.94095	72.51063	76.20008	80.47167	85.98179

TABLE III. PERFORMACE ANALYSIS OF DEVELOPED DR SEGMENTATION AND CLASSIFICATION MODEL WITH EXISTING METHODS

Terms	HHO-HSADMGRNet [28]	SSA-HSADMGRNet[29]	MABOS-HSADMGRNet[30]	GFA-HSADMGRNet[31]	MABGFA HSADMGRNet
Worst	3.408678	4.560688	3.948538	5.15174	2.04325
Best	1.524702	1.641787	1.197277	1.136816	1.189257
Mean	2.400973	2.176032	2.231579	1.696258	1.256214
Median	2.212312	2.325272	1.948192	1.136816	1.189257
Std	0.691964	0.775711	1.040727	0.989689	0.195281

IX. CONCLUSION

A newly developed DR segmentation and classification system is used to detect the DR in the early stage with high accuracy. The retinal fundus images were gathered through resources in internet. The gathered fundus images were given to first stage of pre processing step. Here, the fundus images would be performed by contrast enhancement technique. Then, the pre processed images undergoes to the segmentation section. Here, the pre processed images were segmented by two types of segmentation such as abnormality segmentation and regional segmentation. The abnormality segmentation could be performed using an Adaptive contour-based optic disc removal technique. The regional segmentation could be performed using the Modified U-Net method technique. Then, the segmented images were given to the classification stage. The classification could be done using the HSADMGR Net model. Here, the implemented MABGFA optimization was adapted to optimize the values such as activation function, hidden neuron count and resblock to maximize the precision and accuracy. The suggested MABGFA-HSADMGR Net-based DR classification and segmentation model achieved high performance in terms of F1-score of 13.6% than Mobile Net, 16.1% than Dense net, 14.1% than VGG16, 16% than XGBOOST, 17% than MG_Res net and 15% than RN-Bi-LSTM. The designed HSADMGR Net-based DR segmentation and classification system efficacy was validated among different traditional methods and hybrid algorithms in terms of accuracy and it showed greater performance.

REFERENCES

[1] F. Saeed, M. Hussain and H. A. Aboalsamh, "Automatic Diabetic Retinopathy Diagnosis Using Adaptive Fine-Tuned Convolutional Neural Network," IEEE Access, vol. 9, pp. 41344-41359, 2021.

[2] K. Shankar, Y. Zhang, Y. Liu, L. Wu and C. -H. Chen, "Hyperparameter Tuning Deep Learning for Diabetic Retinopathy Fundus Image Classification," IEEE Access, vol. 8, pp. 118164-118173, 2020.

[3] L. Qiao, Y. Zhu and H. Zhou, "Diabetic Retinopathy Detection Using Prognosis of Microaneurysm and Early Diagnosis System for Non-Proliferative Diabetic Retinopathy Based on Deep Learning Algorithms," IEEE Access, vol. 8, pp. 104292-104302, 2020.

[4] Xiyue Wang, Yuqi Fang, Sen Yang, Delong Zhu, Minghui Wang, Jing Zhang, Jun Zhang, Jun Cheng,"CLC-Net: Contextual and local collaborative network for lesion segmentation in diabetic retinopathy images", Neurocomputing, vol. 527, pp. 100-109, 28 March 2023.

[5] Chenrui Zhang, Ping Chen, Tao Lei, "Multi-point attention-based semi-supervised learning for diabetic retinopathy classification", Biomedical Signal Processing and Control, vol. 80, pp.1044, 12 February 2023.

[6] T. Jemima Jebaseeli, C. Anand Deva Durai, J. Dinesh Peter,"Retinal blood vessel segmentation from diabetic retinopathy images using tandem PCNN model and deep learning based SVM", Optik, vol. 199, pp.163328, December 2019.

[7] Devidas T. Kushnure, Sanjay N. Talbar,"HFRU-Net: High-Level Feature Fusion and Recalibration UNet for Automatic Liver and Tumor Segmentation in CT Images", Computer Methods and Programs in Biomedicine, vol. 213, pp. 106501, January 2022.

[8] Romany F. Mansour, "Deep-learning-based automatic computer-aided diagnosis system for diabetic retinopathy", Biomedical Engineering Letters, vol. 8, p.41–57, 2018.

[9] Sri Laxmi Kuna and Dr.A. V. Krishna Prasad, "An Efficient Meta-Heuristic-Feature Fusion Model using Deep Neuro-Fuzzy Classifier" International Journal of Advanced Computer Science and Applications(ijacsa), 13(11), 2022.

[10] H. Narasimha-Iyer et al., "Robust detection and classification of longitudinal changes in color retinal fundus images for monitoring

diabetic retinopathy," IEEE Transactions on Biomedical Engineering, vol. 53, no. 6, pp. 1084-1098, June 2006.

[11] I. P. Okuwobi, Z. Ji, W. Fan, S. Yuan, L. Bekalo and Q. Chen, "Automated Quantification of Hyperreflective Foci in SD-OCT With Diabetic Retinopathy," IEEE Journal of Biomedical and Health Informatics, vol. 24, no. 4, pp. 1125-1136, April 2020.

[12] K. A. Goatman, A. D. Fleming, S. Philip, G. J. Williams, J. A. Olson and P. F. Sharp, "Detection of New Vessels on the Optic Disc Using Retinal Photographs," IEEE Transactions on Medical Imaging, vol. 30, no. 4, pp. 972-979, April 2011.

[13] L. Seoud, T. Hurtut, J. Chelbi, F. Cheriet and J. M. P. Langlois, "Red Lesion Detection Using Dynamic Shape Features for Diabetic Retinopathy Screening," IEEE Transactions on Medical Imaging, vol. 35, no. 4, pp. 1116-1126, April 2016.

[14] A. Bilal, G. Sun, Y. Li, S. Mazhar and A. Q. Khan, "Diabetic Retinopathy Detection and Classification Using Mixed Models for a Disease Grading Database," IEEE Access, vol. 9, pp. 23544-23553, 2021.

[15] K. Shankar, Y. Zhang, Y. Liu, L. Wu and C. -H. Chen, "Hyperparameter Tuning Deep Learning for Diabetic Retinopathy Fundus Image Classification," IEEE Access, vol. 8, pp. 118164-118173, 2020.

[16] B. Zhang, B. V. K. Vijaya Kumar and D. Zhang, "Detecting Diabetes Mellitus and Nonproliferative Diabetic Retinopathy Using Tongue Color, Texture, and Geometry Features," IEEE Transactions on Biomedical Engineering, vol. 61, no. 2, pp. 491-501, Feb. 2014.

[17] X. Wang et al., "Joint Learning of Multi-Level Tasks for Diabetic Retinopathy Grading on Low-Resolution Fundus Images," IEEE Journal of Biomedical and Health Informatics, vol. 26, no. 5, pp. 2216-2227, May 2022.

[18] K. M. Adal, P. G. van Etten, J. P. Martinez, K. W. Rouwen, K. A. Vermeer and L. J. van Vliet, "An Automated System for the Detection and Classification of Retinal Changes Due to Red Lesions in Longitudinal Fundus Images," IEEE Transactions on Biomedical Engineering, vol. 65, no. 6, pp. 1382-1390, June 2018.

[19] Y. Yang et al., "Robust Collaborative Learning of Patch-Level and Image-Level Annotations for Diabetic Retinopathy Grading From Fundus Image," IEEE Transactions on Cybernetics, vol. 52, no. 11, pp. 11407-11417, Nov. 2022.

[20] S. Qummar et al., "A Deep Learning Ensemble Approach for Diabetic Retinopathy Detection," IEEE Access, vol. 7, pp. 150530-150539, 2019.

[21] A. Osareh, B. Shadgar and R. Markham, "A Computational-Intelligence-Based Approach for Detection of Exudates in Diabetic Retinopathy Images," in IEEE Transactions on Information Technology in Biomedicine, vol. 13, no. 4, pp. 535-545, July 2009.

[22] E. Abdelmaksoud, S. El-Sappagh, S. Barakat, T. Abuhmed and M. Elmogy, "Automatic Diabetic Retinopathy Grading System Based on Detecting Multiple Retinal Lesions," IEEE Access, vol. 9, pp. 15939-15960, 2021.

[23] Sri Laxmi Kuna and A. V. Krishna Prasad, “Deep Learning Empowered Diabetic Retinopathy Detection and Classification using Retinal Fundus Images” International Journal on Recent and Innovation Trends in Computing and Communication ISSN: 2321-8169 Volume: 11Issue:1, 2022 DOI: https://doi.org/10.17762/ijritcc.v11i1.6058.

[24] L. Dai et al., "Clinical Report Guided Retinal Microaneurysm Detection With Multi-Sieving Deep Learning," IEEE Transactions on Medical Imaging, vol. 37, no. 5, pp. 1149-1161, May 2018.

[25] E. O. Rodrigues, A. Conci and P. Liatsis, "ELEMENT: Multi-Modal Retinal Vessel Segmentation Based on a Coupled Region Growing and Machine Learning Approach," IEEE Journal of Biomedical and Health Informatics, vol. 24, no. 12, pp. 3507-3519, Dec. 2020.

[26] Kazem Meidani, Seyedali Mirjalili, and Amir Barati Farimani, "MAB-OS: Multi-Armed Bandits Metaheuristic Optimizer Selection," Applied Soft Computing, vol.128, pp.109452, 2022.

[27] Ritam Guhaa, Soulib Ghosha, Kushal Kanti Ghosha, Ram Sarkara, "Groundwater Flow Algorithm: A Novel Hydro-geologybased Optimization Algorithm," Engineering Optimization, 2020.

[28] H. Pan, Z. Pang, Y. Wang, Y. Wang and L. Chen, "A New Image Recognition and Classification Method Combining Transfer Learning Algorithm and MobileNet Model for Welding Defects," IEEE Access, vol. 8, pp. 119951-119960, 2020.

[29] K. Zhang, Y. Guo, X. Wang, J. Yuan and Q. Ding, "Multiple Feature Reweight DenseNet for Image Classification," IEEE Access, vol. 7, pp. 9872-9880, 2019.

[30] J. Duan and X. Liu, "Online Monitoring of Green Pellet Size Distribution in Haze-Degraded Images Based on VGG16-LU-Net and Haze Judgment," IEEE Transactions on Instrumentation and Measurement, vol. 70, pp. 1-16, 2021.

[31] D. Zhang and Y. Gong, "The Comparison of LightGBM and XGBoost Coupling Factor Analysis and Prediagnosis of Acute Liver Failure," IEEE Access, vol. 8, pp. 220990-221003, 2020.

[32] Z. Zhu et al., "Juggler-ResNet: A Flexible and High-Speed ResNet Optimization Method for Intrusion Detection System in Software-Defined Industrial Networks," IEEE Transactions on Industrial Informatics, vol. 18, no. 6, pp. 4224-4233, June 2022.

[33] R. Zhong, R. Wang, Y. Zou, Z. Hong and M. Hu, "Graph Attention Networks Adjusted Bi-LSTM for Video Summarization," IEEE Signal Processing Letters, vol. 28, pp. 663-667, 2021.

[34] Z. M. Elgamal, N. B. M. Yasin, M. Tubishat, M. Alswaitti and S. Mirjalili, "An Improved Harris Hawks Optimization Algorithm With Simulated Annealing for Feature Selection in the Medical Field," IEEE Access, vol. 8, pp. 186638-186652, 2020.

[35] J. Zhang and J. S. Wang, "Improved Salp Swarm Algorithm Based on Levy Flight and Sine Cosine Operator," IEEE Access, vol. 8, pp. 99740-99771, 2020.

[36] Kuna, Sri Laxmi and Prasad, Dr. A. V. Krishna, Deep Learning Models for Classification of Diabetic Retinopathy Color Fundus Images (September 14, 2022). Available at SSRN: http://dx.doi.org/10.2139/ssrn.4218649.